Reconfigurable-Intelligent-Surface-Assisted MAC for Wireless Networks: Protocol Design, Analysis, and Optimization

Xuelin Cao, Bo Yang, *Member, IEEE*, Hongliang Zhang, *Member, IEEE*, Chongwen Huang, *Member, IEEE*, Chau Yuen, *Fellow, IEEE*, and Zhu Han, *Fellow, IEEE*

Abstract—Reconfigurable intelligent surface (RIS) is a promising reflective radio technology for improving the coverage and rate of future wireless systems by reconfiguring the wireless propagation environment. The current work mainly focuses on the physical layer design of RIS. However, enabling multiple devices to communicate with the assistance of RIS is a crucial challenging problem. Motivated by this, we explore RIS-assisted communications at the medium access control (MAC) layer and propose an RIS-assisted MAC framework. In particular, RIS-assisted transmissions are implemented by prenegotiation and a multidimension reservation (MDR) scheme. Based on this, we investigate RIS-assisted single-channel multiuser (SCMU) communications. Wherein the RIS regarded as a whole unity can be reserved by one user to support the multiple data transmissions, thus achieving high efficient RIS-assisted connections at the user. Moreover, under frequency-selective channels, implementing the MDR scheme on the RIS group division, RIS-assisted multichannel multiuser (MCMU) communications are further explored to improve the service efficiency of the RIS and decrease the computation complexity. Besides, a Markov chain is built based on the proposed RIS-assisted MAC framework to analyze the system performance of SCMU/MCMU. Then the optimization problem is formulated to maximize the overall system capacity of SCMU/MCMU with energy-efficient constraint. The performance evaluations demonstrate the feasibility and effectiveness of each.

I. Introduction

THE EMERGENCE of the Internet-of-Everything (IoE) system, the rapid development of data-centric and automated processes have extended the coverage of mobile communications from the legacy interpersonal communication to smart interconnection among millions of people and billions of devices. These devices are spurring worldwide activities focused on defining the next-generation wireless communications that can truly meet the demands for a fully connected and intelligent digital world [1], [2]. Currently, important 5G and beyond technologies, such as Internet-of-Things (IoT) paradigm have received much attention in academia and industry, which brings considerable challenges and opportunities in the fundamental architecture, the performance of the component, and especially for the standards at the medium access control (MAC) layer [3], [4]. It is admitted that the ongoing unprecedented proliferation of intelligent communication is posing new challenges to MAC that needs to cater to low energy consumption, low cost, high intelligence, high capacity, and easy implementation.

Recently, the reconfigurable intelligent surface (RIS) that also is known as intelligence reflecting surface or holographic multiple input multiple output surface (HMIMOS) [5], [6] has been envisioned as intrinsic components of beyond 5G wireless systems to offer unprecedented spectral efficiency gains and drive the wireless architectural evolution [7]–[9]. The core concept of RIS is stacking a massive number of passive radiating elements to realize a continuous electromagnetically active surface. RIS technology has been verified as an alternative to beamforming techniques since RIS can tune the phase of the incident signal by the intelligent reflection of elements without buffering or processing [10]. In that way, the reflected signal from RIS can be aligned with the nonreflected signal at the receiver to enhance the communication performance and improve the coverage of the wireless systems [11]–[16]. In other words, manipulating the reflection characteristics of the RIS can improve the propagation condition, enrich the communication channel, and increase the energy efficiency.

The most existing works focused on the RIS beamforming design considering the global channel state information (CSI) [17]–[27]. Basar [17], [18] proposed the RIS-aided transmission strategy index modulation to improve the system spectral efficiency. Wu and Zhang [21] studied the joint optimization problem of active and passive beamforming. Guo *et al.* [22] studied an RIS-aided multiuser system to maximize the weighted sum rate by joint designing the beamforming and the RIS phase shift. Huang *et al.* [23]–[25] aimed to maximize the sum rate and energy efficiency of RIS-assisted multiuser downlink system. Abeywickrama *et al.* [26] investigated the RIS system that can capture the phase-dependent amplitude variation in the elementwise reflection coefficient. Han *et al.* [27] evaluated the performance of a LIS-assisted large-scale antenna system with different propagation scenarios. Even more recently, RIS-assisted uplink multiuser system and RIS-assisted physical-layer security schemes were discussed in [28]–[30]. Besides the theoretic analysis of RIS, the RIS prototype has been developed in [31], which combines the functions of phase shift and radiation together on an electromagnetic surface, positive intrinsic-negative (PIN) diodes are used to realize 2-bit phase shifting for beamforming.

A. Challenges and Motivations

Different from the various existing MAC [32]–[34], we focus on designing MAC with the assistance of the RIS. It is generally known that the achievable RIS techniques in the physical layer have shown a profound potential in future wireless communications, which inspires a feasibility solution on RIS enabling in the MAC layer. However, utilizing RIS to serve multiple users' transmissions at the MAC layer still faces some challenges, such as 1) how to construct RIS-assisted communications for the multiuser system; 2) how to avoid interference at the receiver caused by RIS reflection; and 3) how to jointly optimize the RIS configuration and MAC layer parameters. These issues cannot be addressed by directly applying the existing MAC schemes, to the authors' best knowledge.

Motivated by the challenges raised, in this article, we mainly focus on the compatible design of RIS-assisted MAC by taking the following measures.

1) To address challenge 1), we design a novel RIS-assisted MAC framework, where the negotiation and data transmission are fit together in a hybrid way. During the negotiation phase, each user acquires the RIS resources to assist its data transmissions in a distributed way. This kind of design is especially applicable in the IoT system that pursues spectrum efficient and energy efficient.

2) To address challenge 2), we propose the multidimension reservation (MDR) scheme for each user. Using the MDR scheme, each user can reserve the RIS resources in advance to achieve multiple RIS-assisted data transmissions without interference during the transmission phase, thus improving the RIS elements utilization.

3) To address challenge 3), we formulate a joint optimization problem for RIS-assisted communications with considering RIS configuration, transmission power, and MAC parameters to maximize the system capacity.

Moreover, the proposed MAC framework is feasibly implemented in practice. Specifically, it is known that the mature medium access schemes [e.g., carrier-sense multiple access with collision avoidance (CSMA/CA) and time-division multiple access (TDMA)] have already been implemented in the commercial off-the-shelf (COTS) products, which may not be likely modified. Therefore, the proposed MAC framework can use the RIS elements efficiently with low complexity, which shows the significance of practical implementation.

B. Contributions

In the article, the main contributions are summarized as follows.

1) *RIS-Assisted MAC Framework:* We propose an RIS-assisted MAC framework for the multiuser uplink system. In this framework, we separate the negotiation and RIS-assisted data transmissions in the time domain using the MDR scheme, and we solve the RIS elements allocation issue at the MAC layer to avoid interference.

2) *RIS-Assisted SCMU/MCMU Communications:* We explore RIS-assisted single-channel multiuser (SCMU) communications based on the proposed RIS-assisted MAC framework. With the implementation of the SCMU, the RIS serves one user at a time for completing the energy-efficient transmission. By introducing the RIS group division, we then further extend to RIS-assisted multichannel multiuser (MCMU) communications to support concurrent transmissions via the RIS.

3) *Analysis of RIS-Assisted SCMU/MCMU Communications:* We construct a Markov model to analyze the system performance of RIS-assisted SCMU/MCMU communications. Unlike the existing analysis, we separate the contention process and RIS-assisted data transmissions in the time domain. Accordingly, we introduce the contention state and the transmission state, which correspond to the negotiation period and the data transmission period of the proposed RIS-assisted MAC framework, respectively.

4) *Optimization and Simulation Results:* We formulate the joint optimization problems to maximize the system capacity of RIS-assisted SCMU/MCMU communications with considering RIS configuration, transmit power, and MAC parameters. Moreover, we conduct the simulations on RIS-assisted SCMU/MCMU communications and demonstrate the performance of both in terms of system throughput, signal-to-noise ratio (SNR), and transmit power.

C. Organization and Notations

The remainder of this article is organized as follows. In Section II, RIS-assisted communications system model is presented. Section III proposes an RIS-assisted MAC framework. Sections IV and V investigate how to implement the proposed RIS-assisted MAC framework in SCMU communications and MCMU communications, respectively. In Section VI, performance evaluation is presented. Finally, Section VII concludes this article.

TABLE I
LIST OF NOTATION

Notation	Definition
N	The number of RIS elements
K	The number of users
U_k	User k
h_k	The direct channel from U_k to AP
$\mathbf{G_k}$	The channel from U_k to the RIS
$\mathbf{H_k}$	The channel from the RIS to AP for U_k
$\mathbf{\Theta_k}$	Phase-shift matrix of the RIS for U_k
s_k	Signal from U_k
θ_k^n	Phase-shift of element n for U_k
β_k^n	Amplitude reflection coefficient of element n for U_k
ρ_k^2	The transmitter power at U_k with the RIS
SNR_k	Signal-to-noise ration at AP from U_k
Γ_k	The received power at AP from U_k via the RIS
d_k	The distance between U_k and AP
$d_k^{1,n}$	The distance between element n and U_k
$d_k^{2,n}$	The distance between element n and AP
P_{RIS}	The hardware static power consumption at the RIS
$P_{k,c}$	The total power consumption at U_k with the RIS
P	The transmit power at any U_k without the RIS
T_k^{ini}	Initial data transmission time of U_k
T_{cycle}	The data transmission cycle
r_k	The number of reserved transmissions of U_k
$\{W, s\}$	Backoff value
γ	The transmission rate from "C" to "T"
η	The transmission rate from "T" to "C"
p	The stationary probability that a user keeps in "C"
q	The collision probability while one user transmits
τ	The probability that one user transmits in a slot
ζ_s	The probability of successful transmission
ζ_e	The probability of idle channel
ζ_c	The probability of collision
t_s	The time of successful negotiation
t_c	The time of collision
T	The length of a frame
t_h	The length of the negotiation period
t_r	The length of RIS-assisted transmission period
R_k	The achievable data rate at U_k
$\Im_{Total}$	The total capacity
ε_k	The probability that U_k transmits in one frame
$A_x : A_y$	The size of RIS
$l_x : l_y$	The size of RIS group
L	The number of RIS groups
C	The number of sub-channels
B	The channel bandwidth
$\pi(j)$	The steady-state probability with j used sub-channels

Notation: For ease of reference, Table I summarizes the main notations used throughout this article. Furthermore, $\mathbb{C}^{x*y}$ represents a $x*y$ complex-valued matrix. diag($\mathbf{z}$) is a diagonal matrix with its diagonal elements given in vector $\mathbf{z}$.

II. RIS-ASSISTED COMMUNICATIONS SYSTEM MODEL

In this section, the system scenario, the channel model, and the propagation model are presented, where the PHY layer

aspects are introduced since we design the suitable MAC based on the RIS physical layer characteristics [35], [36].

A. System Scenario

We consider a multiuser uplink wireless system, where the RIS is attached with an RIS controller that can be controlled by the AP via a separate wireless link [23]. The RIS consists of N passive elements and can be further divided into L groups. The L RIS groups are bonded with C subchannels that can be used to assist the communication of K users (i.e., $U_k, k \in [1, K]$) with one AP. The channels from the U_k to the RIS, from the RIS to the AP, and from the U_k to the AP are denoted by the set $\mathbf{G}_k = \{G_k^1, \ldots, G_k^n, \ldots, G_K^{N/L}\}$, the set $\mathbf{H}_k = \{H_k^1, \ldots, H_k^n, \ldots, H_K^{N/L}\}$, and h_k, respectively, where $\mathbf{G}_k \in \mathbb{C}^{(N/L)\times 1}$ and $\mathbf{H}_k \in \mathbb{C}^{1\times(N/L)}$. Besides, the communication bandwidth is B, and the occupied bandwidth by each subchannel is B/C. We mainly focus on the uplink channel access of multiple users with the assistance of RIS. Note that each RIS element is just allowed to support one user's transmission and reflect its signal to AP at one time. Otherwise, interference occurs. According to the value of C and L, the system model in Fig. 1 can be classified into two cases as follows: when 1) $C = 1$ and 2) $L = 1$, RIS-assisted SCMU communications are shown in Fig. 1(a), where all RIS elements serve one user at a time on one channel. On the other hand, as $C > 1$ and $L > 1$, RIS-assisted MCMU communications are shown in Fig. 1(b), where L RIS groups serve multiple users at a time on C subchannels.

B. Channel Model

Based on the RIS channel model, the received signal at AP from U_k in RIS-assisted SCMU/MCMU communications can be denoted by

$$y_k^{SCMU} = \underbrace{h_k s_k}_{\text{Direct data link}} + \underbrace{\mathbf{H}_k \mathbf{\Theta}_k \mathbf{G}_k s_k}_{\text{RIS-assisted data link}} + w_k \qquad (1)$$

and

$$y_k^{MCMU} = \underbrace{h_k s_k}_{\text{Direct data link}} + \underbrace{\mathbf{H}_k^l \mathbf{\Theta}_k^l \mathbf{G}_k^l s_k}_{\text{RIS-groups-assisted data link}} + w_k \qquad (2)$$

where s_k represents the signal from U_k, which is identically distributed (i.i.d.) random variable with zero mean and unit variance, w_k is additive white Gaussian noise (AWGN) of U_k at AP with zero mean and variance σ^2. For RIS-assisted transmission channel in (1) and (2), $\mathbf{\Theta}_k$ and $\mathbf{\Theta}_k^l$ can be defined as

$$\mathbf{\Theta}_k = \text{diag}\left(\phi_k^1, \ldots, \phi_k^n, \ldots, \phi_k^N\right) \qquad (3)$$

and

$$\mathbf{\Theta}_k^l = \text{diag}\left(\phi_k^{l(1)}, \ldots, \phi_k^{l(n)}, \ldots, \phi_k^{l(N/L)}\right). \qquad (4)$$

Let $\phi_k^n = \beta_k^n e^{j\theta_k^n}, n \in [1, N]$ and $\phi_k^{l(n)} = \beta_k^{l(n)} e^{j\theta_k^{l(n)}}, l(n) \in [1, N/L]$ denote the phase shift of each element n on the RIS group l for U_k, where $\{\theta_k^n, \beta_k^n\}$ and $\{\theta_k^{l(n)}, \beta_k^{l(n)}\}$ are the phase shift and amplitude reflection coefficient of element n on the RIS group l for U_k, respectively. In practice, considering the
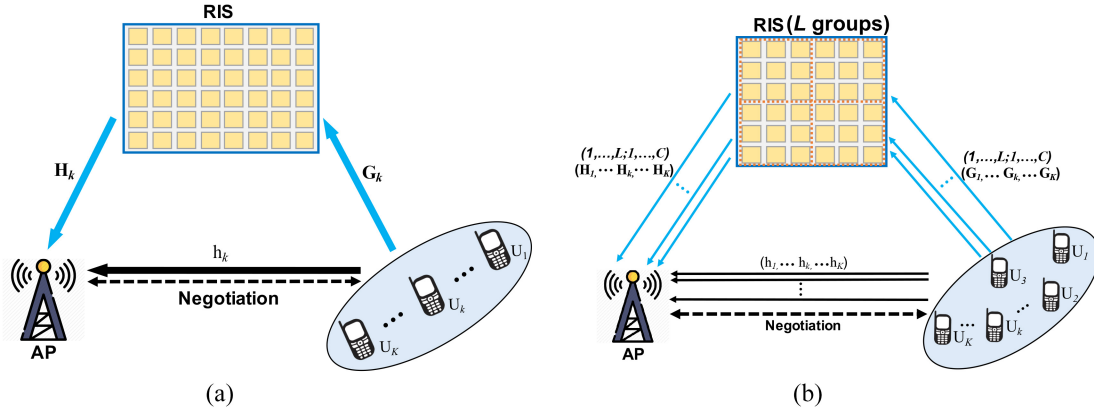
Fig. 1.   RIS-assisted SCMU/MCMU communications system model. (a) RIS-assisted SCMU communications. (b) RIS-assisted MCMU communications.
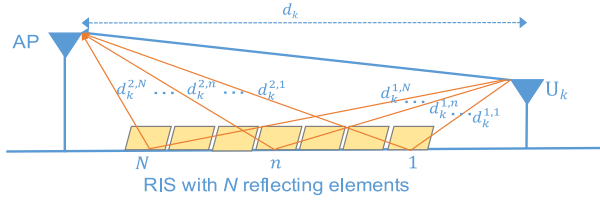

Fig. 2.   Reflection-based propagation model via the RIS.

hardware implementation, we assume that the discrete phase shift with constant amplitude is operated on each RIS element. Then, we have

$$\phi_k = \left\{ \phi_k^n | \phi_k^n = e^{j\theta_k^n}, \theta_k^n \in \mathbf{\Omega} \quad \forall n \right\} \tag{5}$$

and

$$\phi_k^{l(n)} = \left\{ \phi_k^{l(n)} | \phi_k^{l(n)} = e^{j\theta_k^{l(n)}}, \theta_k^{l(n)} \in \mathbf{\Omega} \quad \forall n \right\}. \tag{6}$$

Without loss of generality, denote by b the number of bits used to represent each of the levels, and then the set of phase shifts at each element, $\mathbf{\Omega}$, is given by $\mathbf{\Omega} = \{0, \Delta\theta, \dots, \Delta\theta(\Psi - 1)\}$, where $\Delta\theta = 2\pi/\Psi$, and $\Psi = 2^b$ denotes the number of quantized reflection coefficients values of RIS elements. To achieve the best signal reflection, the RIS controller should adjust its reflection coefficient to make the reflected signals coherently added at AP deliberately.

Let ρ_k^2 be the transmitter power from U_k to AP, the received SNR at the AP from U_k in RIS-assisted SCMU/MCMU communications can be calculated as

$$\text{SNR}_k^{\text{SCMU}} = |(h_k + \mathbf{H}_k \mathbf{\Theta}_k \mathbf{G}_k)\rho_k|^2/\sigma^2 \tag{7}$$

and

$$\text{SNR}_k^{\text{MCMU}} = \left| \left(h_k + \mathbf{H}_k^l \mathbf{\Theta}_k^l \mathbf{G}_k^l \right)\rho_k \right|^2/\sigma^2. \tag{8}$$

C. Propagation Model

The motivation of the RIS is to control the radio environment, where the wireless channel can be turned into a deterministic by reconfiguring the propagation of the electromagnetic wave in a software-controlled fashion. The reflection-based propagation model via the RIS in a free-space

environment is shown in Fig. 2. The received power at AP from U_k through the RIS link can be obtained as

$$\Gamma_k = \rho_k^2 \left(\frac{\lambda}{4\pi} \right)^2 \left| \frac{1}{d_k} + \sum_{n=1}^{N} \frac{\phi_k^n \times e^{-j\Delta\theta_k^n}}{d_k^{1,n} + d_k^{2,n}} \right|^2 \tag{9}$$

where λ is the wavelength, d_k is the distance of direct link from U_k to AP. The distance between the U_k and the RIS element n, and the RIS element n and AP are denoted by $d_k^{1,n}$ and $d_k^{2,n}$, respectively. Moreover, $\Delta\theta_k^n = ([2\pi(d_k^{1,n} + d_k^{2,n} - d_k)]/\lambda)$ is the phase difference between the RIS link and the direct link. When d_k is sufficiently large, we can assume $d_k = d_k^{1,n} + d_k^{2,n}$ $\forall n \in [1, N]$. To achieve the best performance of the RIS, the phase shift of each RIS element is aligned with the phase of the LOS path. Considering this ideal case, (9) can be rewritten as follows:

$$\Gamma_k \approx (N+1)^2 \rho_k^2 \left(\frac{\lambda}{4\pi d_k} \right)^2 \tag{10}$$

then the received power at AP from U_k can be simplified as follows:

$$\Gamma_k \propto N^2 \rho_k^2 \left(\frac{1}{d_k} \right)^2 \tag{11}$$

which shows that the received power at the AP is proportional to N^2 and is inversely proportional to d_k^2. In other words, the number of RIS elements can affect the power gain and thus displays potential in low power and data-intensive wireless communications. Note that $\Gamma_k \propto \rho_k^2 (1/d_k)^2$ holds if RIS is not used, i.e., the part that $\sum_{n=1}^{N}([\phi_k^n \times e^{-j\Delta\theta_k^n}]/[d_k^{1,n} + d_k^{2,n}])$ in (9) can be removed. This can be viewed as a direct link channel model.

Therefore, the total power consumption of the $U_k \rightarrow$ RIS $\rightarrow$ AP link can be given as

$$P_{k,c} = \rho_k^2 + P_{\text{RIS}} + \Gamma_k \tag{12}$$

where P_{RIS} is the hardware static power consumption at the RIS, ρ_k^2 is the transmit power at U_k, and Γ_k is the revived power at AP from U_k. If the RIS is not used, only direct link $U_k \rightarrow$ AP exists, the total power consumption of the direct link is $P + \Gamma_k$, where P represents the transmit power of any user without using the RIS. In other words, the transmit power P can enable the AP to receive the signal from any user.
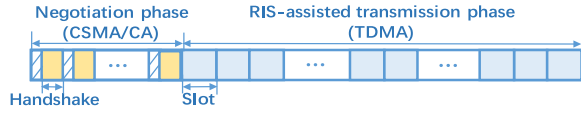
Fig. 3.   RIS-assisted MAC framework.

III. RIS-ASSISTED MAC FRAMEWORK

In the multiuser uplink communications system, an RIS-assisted MAC framework is designed in Fig. 3. Following the CSMA scheme, each user proposes the uplink transmissions and reserves the RIS resources (i.e., the RIS elements). The AP estimates the channels of the direct link and RIS links, and controls the RIS to assist each user's uplink data transmissions in TDMA mode. The detailed work on the channel estimation can refer to the related [37], [38].

1) Frame Structure: The frame is shown in Fig. 3, where each frame is separated into two phases: 1) the negotiation phase and 2) the RIS-assisted transmission phase [39]. The RIS-assisted transmission phase can be further divided into a series of slots. In the negotiation phase, each user competes for the access privilege according to the backoff mechanism and then negotiates with the AP to reserve the RIS resources, power resources, channel resources, and slot resources. As the RIS-assisted transmission phase arrives, the RIS can be controlled and switched to the requested users on the negotiated channels and slots.

2) MDR Scheme: MDR is proposed in the negotiation phase to implement RIS-assisted data transmissions. Each dimension is defined as one type of reservation information.

1) *Dimension 1 (D1) (Time Zone):* The slots that are in the RIS-assisted transmission phase can be reserved on the channel;
2) *Dimension 2 (D2) (Power Zone):* The transmit power can be used at the requested user while starting RIS-assisted data transmissions;
3) *Dimension 3 (D3) (RIS Zone):* The phase shift of each RIS element, which can be controlled by the AP to align with the user's direct data transmission in the RIS-assisted transmission phase.
4) *Dimension 4 (D4) (Frequency Zone):* The subchannel and the corresponding RIS group are requested by the user at the negotiation phase for data transmission at the RIS-assisted transmission phase. Note that one subchannel is bonded with one RIS group. Once the subchannel is reserved, the accordingly RIS group is reserved;

3) Extended Control Packets: Two types of extended control packets are introduced to implement the MDR scheme, i.e., extended request to send (eRTS) and extended clear to send (eCTS). The control packet structure of each is shown as follows.

1) *eRTS* (T_k^{ini}, r_k, T_{cycle}, c_k, l_k) *of* $U_k, k \in [1, K]$: eRTS is an extension of the traditional RTS packet defined in IEEE 802.11 DCF. Compared to RTS, five additional fields, i.e., the initial transmission time (T_k^{ini}), the transmission cycle (T_{cycle}), the number of reserved transmissions (r_k), the subchannel (c_k) and the RIS group (l_k), are added into the eRTS. Note that the fields of c_k and l_k are omitted in RIS-assisted SCMU communications.

2) *eCTS* ($\rho_k{}^2$, T_k^{ini}, r_k, T_{cycle}, c_k, l_k) *of* $U_k, k \in [1, K]$: eCTS is an extension of the traditional CTS packet defined in IEEE 802.11 DCF. Compared to CTS, six additional fields, i.e., the transmission power($\rho_k{}^2$), T_k^{ini}, T_{cycle}, r_k, c_k and l_k, are added into the eCTS. Note that the fields of c_k and l_k are omitted in RIS-assisted SCMU communications.

IV. RIS-ASSISTED SCMU COMMUNICATIONS

In this section, as shown in Fig. 1(a), we explore how to implement RIS-assisted SCMU communications for the multiuser uplink communications system, where only one channel is considered, and all RIS elements serve one user (i.e., $L = 1$ and $C = 1$).

A. Basic Idea

The proposed RIS-assisted SCMU communications are shown in Fig. 4. Based on the proposed RIS-assisted MAC framework, the three-dimension reservation that includes D1, D2, and D3 is introduced in the negotiation phase, wherein each user competes for the channel to reserve the available slots and RIS elements with AP. AP calculates the RIS reflection coefficients and the transmit power for the requested user and then informs them of the data transmission during the RIS-assisted transmission period. Once the mentioned three-dimension reservation is constructed, the requested user commences its transmissions in the reserved slots with the reserved transmit power, and the RIS controller adjusts the phase shift of each RIS element at the reserved slots to assist the requested user's transmissions. In RIS-assisted SCMU communications, since the RIS controller updates all RIS elements' reflection coefficients for one user at one time, the complexity of RIS phase-shift adjustment is $\mathcal{O}(N)$.

B. Implementation Algorithm

The implementation algorithm of RIS-assisted SCMU communications is presented in Algorithm 1. Considering the uplink traffics of $U_k, k \in [1, K]$, Algorithm 1 contains two phases.

1) Phase 1 (Negotiation Phase):

1) *Step 1:* The requested user competes for the channel by operating the backoff scheme during the negotiation period, i.e., each user sets its backoff value $\{W, s\}$, where $W \in [CW_{min}, CW_{max}]$ and $s \in [0, m]$ denote the backoff counter and the backoff stage, respectively. CW_{min} and CW_{max} are the minimum contention window and maximum contention window, m is the maximum backoff stage. Once the channel is sensed to be idle, each user decreases W by one after a slot. Once the user decreases W to zero, it wins the channel access privilege. If a collision occurs, the value of s increases by one until $s = m$.

2) *Step 2:* By sending the eRTS packet to the AP with the power P, U_k requests its T_k^{ini}, T_{cycle}, and r_k from AP for its multiple RIS-assisted transmissions. Besides, the other users keep silent by setting the network allocation vector (NAV) when U_k is negotiating with the AP.
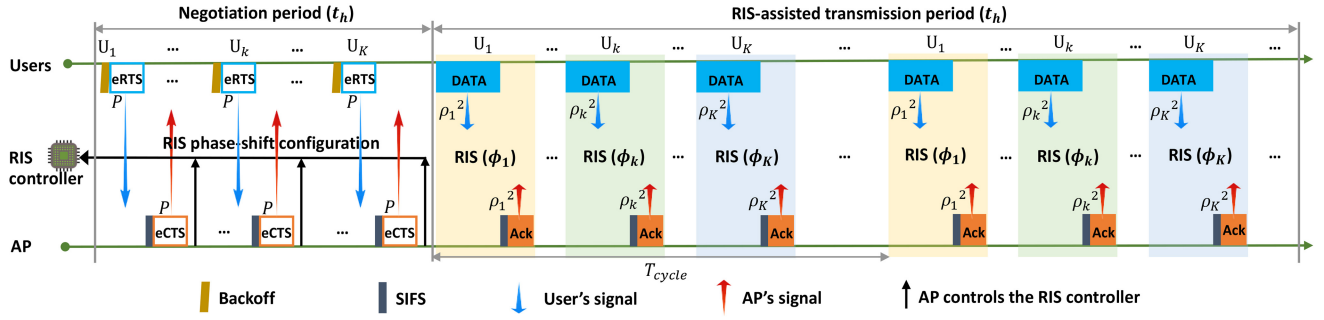
Fig. 4. RIS-assisted SCMU communications, where $L = 1$ and $C = 1$. Each user contends the access privilege and negotiates with AP (i.e., eRTS/eCTS exchanging) in a single channel.

3) *Step 3:* On receiving the eRTS packet, if no collision occurs on the reserved RIS and slots, the AP estimates the phase shift of each RIS element, ϕ_k, and calculates the transmit power, ρ_k^2, at U_k as well. Besides, the AP records ρ_k^2, T_k^{ini}, r_k and T_{cycle} into the eCTS packet, and replies it to U_k while notifying the ϕ_k, T_k^{ini}, r_k and T_{cycle} to the RIS controller. Otherwise, the AP uses a new value T_k^{ini*} instead of T_k^{ini} in the eCTS packet, and replies it to U_k while notifying the RIS controller.

4) *Step 4:* Once U_k receives the eCTS packet from the AP, U_k ceases its competition in the current negotiation period and waits for the RIS-assisted transmission phase. When the NAV expired out, other requested users continue the backoff procedure until the negotiation period terminates.

2) *Phase 2 (RIS-Assisted Transmission Phase):*

1) *Step 1:* When the reserved slots arrive, U_k sends the data with the transmit power, ρ_k^2. Meanwhile, RIS controller sets the phase shift of each RIS element as θ_k^n, $\theta_k^n \in \mathbf{\Omega}$ $\forall n \in [1, N]$, and reflects U_k's signal to the AP.

2) *Step 2:* On receiving the accumulated reflected signal from the RIS and the LOS's signal from U_k correctly, the AP replies an ACK packet to U_k.

3) *Step 3:* During RIS-assisted transmissions between U_k and AP, other users set the NAV to cease their transmissions until the reserved RIS-assisted transmissions of U_k finishes.

C. Performance Analysis

In this section, a two-state transition model [40] is illustrated for the proposed RIS-assisted MAC framework, where each user maintains two states: 1) the contention state "C" and 2) the transmission state "T." Let γ and η denote the transmission rate from "C" to "T" and from "T" to "C," respectively. Then, the stationary probability of two states can be given as

$$\mho \triangleq (q, 1 - q) = \left(\frac{\eta}{\gamma + \eta}, \frac{\gamma}{\gamma + \eta} \right) \tag{13}$$

where q and $1 - q$ represent the stationary probability that a user keeps in the state of "C" and "T," respectively.

The two-state transition model, combined with the traditional backoff process, is constructed in Fig. 5, which is different from Bianchi's model [41] since the contention and the data transmission are separated. Specifically, the state "C" corresponds to the negotiation period, and the state "T" corresponds to the data transmission period of the proposed RIS-assisted MAC framework. In our model, each contention state of user is denoted by (s, W), where $s \in [0, m]$ and $W \in [0, W_m]$ denote the backoff stage and the backoff counter, respectively. Then, we can get

$$\begin{cases} 1) \ P_{s,W|s,W+1} = 1, & W \in [0, W_s - 2], \ s \in [0, m] \\ 2) \ P_{0,W|s,0} = q(1-p)/W_0, & W \in [0, W_0 - 1], \ s \in [0, m] \\ 3) \ P_{s,W|s-1,0} = p/W_s, & W \in [0, W_s - 1], \ s \in [1, m] \\ 4) \ P_{m,W|m,0} = p/W_m, & W \in [0, W_m - 1] \\ 5) \ P_{T|s,0} = (1-q)(1-p), & s \in [0, m] \\ 6) \ P_{0,W|T} = q/W_0, & W \in [0, W_0 - 1] \\ 7) \ P_{T|T} = 1 - q \end{cases} \tag{14}$$

where p is the probability that a collision happen while one user transmits. $W_s = 2^s W_0$ is the contention window when backoff stage is s, where W_0 denotes the minimum contention window. Expressions 1)–4) in (14) describe the backoff process when users stay in the state of "C," the remaining expressions 5)–7) show that the reserved transmission process when users keep the state of "T." Specifically, expression 1) means that the backoff counter is decremented one with probability 1. Expression 2) is explained that a new packet following a successful packet transmission begins a new backoff process with probability $q(1-p)/W_0$, here, s is valued 0, W is reset in the range $(0, W_0 - 1)$. Expression 3) shows that an unsuccessful transmission occurs at the backoff stage of $s - 1$, the backoff stage is increased one (i.e., backoff stage become s), and a new initial backoff counter value is uniformly selected in the range $(0, W_s)$. Expression 4) illustrates that once s equals to the maximum value m, it is not increased in subsequent

$$\tau = \frac{2(1 - 2p)q}{q\left[(CW_0 + 1)(1 - 2p) + pCW_0(1 - (2p)^m) \right] + 2(1 - q)(1 - p)(1 - 2p)} \tag{15}$$

Algorithm 1: RIS-Assisted SCMU Communications

1   Initialize $|\phi_k^n| = 0$, $\rho_k^2 = P$ $\forall j, k \in [1, K]$;
2   $t = 0$;
3   **Phase 1: Negotiation phase**;
4   **if** t is in **Phase 1 then**
5   **if** U_k has data to transmit **then**
6   U_k sets its backoff value $\{W, s\}$;
7   **if** $W = 0$ **then**
8   U_k sends eRTS to AP;
9         $U_{j,j \neq k}$ sets NAV and keeps silent;
10   AP receives eRTS and judges;
11   **if** *no collision* **then**
12   AP calculates ϕ_k, ρ_k^2;
13   AP replies eCTS to U_k;
14   Ap notifies the RIS controller about the $\phi_k, T_k^{ini}, r_k, T_{cycle}$;
15   **end**
16   **else**
17   AP replies eCTS to U_k;
18   AP notifies the RIS controller about the $\phi_k, T_k^{ini*}, r_k, T_{cycle}$;
19   **end**
20   U_k receives eCTS and waits for **Phase 2**;
21   **end**
22   **else**
23         $W--$;
24   **end**
25   **end**
26   **else**
27   U_k keeps silent;
28   **end**
29   **end**
30   **else**
31   U_k waits for **Phase 1**;
32   **end**
33   **Phase 2: RIS-assisted transmission phase**;
34   **if** t is in **Phase 2 then**
35   U_k transmits data to AP at the reserved slots with power ρ_k^2;
36   RIS controller sets ϕ_k and reflects U_k's signal;
37   AP receives reflected and directed signals from U_k;
38   AP replies ACK to U_k;
39   **end**
40   **else**
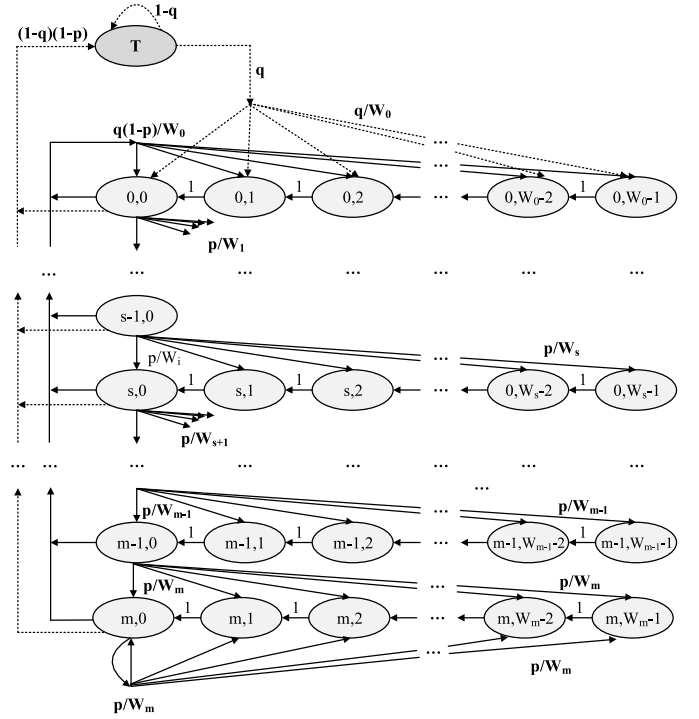41 U_k waits for **Phase 2**;
42   **end**

Fig. 5. Enhanced discrete Markov model based on the two-state transition.

period). Here, γ and η can be calculated as

$$\begin{cases} \gamma = \frac{\zeta_s}{\zeta_e \delta + \zeta_s t_s + \zeta_c t_c} \\ \eta = \frac{1}{t_p r_{\max}} \end{cases} \tag{16}$$

where $t_s = eRTS + eCTS + DIFS + SIFS$, δ and $t_c = eRTS + DIFS$ represent the time duration of successful negotiation, idle state and collision, respectively. Here, *eRTS* and *eCTS* are the transmissions time of the eRTS packet and the eCTS packet, respectively. *DIFS* and *SIFS* are the duration of DIFS and SIFS, respectively. t_p denotes the time length of one data transmission, and $r_{\max}$ is the maximum number of reserved transmission which equals to (t_r/T_{cycle}). ζ_s, ζ_e and ζ_c represent the probability of successful RIS-assisted transmission, the probability of idle channel and the probability of collision, respectively, which are given as

$$\begin{cases} \zeta_s = Kq\tau(1 - \tau)^{Kq-1} \\ \zeta_e = (1 - \tau)^{Kq} \\ \zeta_c = 1 - \zeta_s - \zeta_e. \end{cases} \tag{17}$$

To improve the channel utilization, we suggest $T_{cycle} = N_r * t_p$, i.e., a guideline for setting T_{cycle} in the proposed RIS-assisted SCMU/MCMU communications, where N_r can be approximately calculated by $\lfloor [t_h \zeta_s]/t_s \rfloor$. When t_p is given, a large T_{cycle} means that a big N_r, which brings the more overheads. Note that if the number of data packets accumulated at the MAC queue is larger than $r_{\max}$, the user needs to contend again in the next negotiation phase.

According to (7), the achievable data rate at U_k can be given by

$$R_k^{\text{SCMU}}(\rho_k, \phi_k) = B \log_2 \left(1 + \text{SNR}_k^{\text{SCMU}} \right) \tag{18}$$

where B is the channel bandwidth.

packet transmissions. Expression 5) models the fact that a successful packet transmission switches from contention state to transmission state with probability $(1-q)(1-p)$, and expression 6) illustrates the user switches into contention state from transmission state with probability q/W_0. Finally, expression 7) shows that users maintain its original state of "T" with probability $1 - q$.

In the proposed RIS-assisted MAC framework, since the MDR scheme is introduced into the access process of each user, the stationary probability that one user transmits a data packet in a random slot during the RIS-assisted transmission phase, τ, is given by (15), shown at the bottom of the previous page. In (15), $p = 1 - (1 - \tau)^{Kq-1}$ is the collision probability and $q = \eta/(\gamma + \eta)$ is the stationary probability that one user stays in the state of "C" (i.e., the user locates in the negotiation

The total capacity of RIS-assisted SCMU communications can be calculated as follows:

$$\Im_{\text{Total}}^{\text{SCMU}} = \sum_{k=1}^{K} \frac{t_p r_k}{T} \varepsilon_k R_k^{\text{SCMU}}(\rho_k, \phi_k)$$

$$= \frac{t_p}{T} B \sum_{k=1}^{K} r_k \varepsilon_k \log_2\left(1 + \text{SNR}_k^{\text{SCMU}}\right) \quad (19)$$

where r_k is the number of data transmissions at U_k in the RIS-assisted transmission phase. $T = t_h + t_r$ are the length of a frame, where t_h and t_r are the length of the negotiation period and the length of the RIS-assisted transmission period, respectively. t_p is the time length of one data transmission, and $t_p r_k$ denotes the time length of r_k data transmissions at U_k in the RIS-assisted transmission phase. $\varepsilon_k = ([t_h \zeta_s]/t_s K)$ is the probability that U_k commences its data transmissions during the RIS-assisted transmission period. $\text{SNR}_k^{\text{SCMU}}$ is the SNR at U_k with RIS-assisted SCMU communications. Given the fixed value of ε_k, (19) can be written as

$$\Im_{\text{Total}}^{\text{SCMU}} = \frac{t_p t_h \zeta_s}{T t_s K} B \sum_{k=1}^{K} r_k \log_2\left(1 + \text{SNR}_k^{\text{SCMU}}\right). \quad (20)$$

D. Performance Optimization

Based on the aforementioned performance analysis of the RIS-assisted MAC framework, the performance optimization for RIS-assisted SCMU communications can be formulated as

$$\textbf{P1}: \quad \max_{\rho_1^2, \dots, \rho_K^2; \Theta_1, \dots, \Theta_K; r_1 \dots, r_K} \Im_{\text{Total}}^{\text{SCMU}}$$

$$\text{s.t.} \quad \text{C1}: \ 0 \le \rho_k^2 \le P - P_{\text{RIS}} \quad \forall k$$
$$\text{C2}: \ |\phi_k^n| = 1 \quad \forall k, n$$
$$\text{C3}: \ \theta_k^n \in \Omega \quad \forall k, n$$
$$\text{C4}: \ t_h + t_r = T \quad \forall k$$
$$\text{C5}: \ \frac{t_p}{t_s} r_{\max} \zeta_s \le \frac{t_r}{t_h} \quad \forall k$$
$$\text{C6}: \ 1 \le r_k \le r_{\max} \quad \forall k \quad (21)$$

where C1 constrains the transmit power of each user. C2 and C3 separately illustrate the constraints of the amplitude and phase shift of RIS elements. Constraint C4 constrains the length of a frame, and C5 constrains the RIS-assisted transmission period and the negotiation period. Constraint C6 limits the number of data transmissions.

In (19), since $([t_p t_h \zeta_s]/T t_s K)B$ is constant, problem P1 can be transformed to (22), i.e.,

$$\textbf{P2}: \quad \max_{\rho_1^2, \dots, \rho_K^2; \Theta_1, \dots, \Theta_K; r_1 \dots, r_K} \sum_{k=1}^{K} r_k \log_2\left(1 + \text{SNR}_k^{\text{SCMU}}\right)$$

$$\text{s.t.} \quad \text{C1} - \text{C6}. \quad (22)$$

Since problem P2 is a nonconvex optimization problem, it makes the solution difficult to achieve. The alternating-based method is used to solve it, problem P2 can be split into two subproblems as follows.

1) Fixed Value of $r_1, \dots, r_K$: Problem P2 can be simplified as subproblem P2.1, where the phase shift of each RIS element can be optimized to maximize the SNR of each user, which is shown as

$$\textbf{P2.1}: \quad \max_{\rho_k^2; \Theta_k} \text{SNR}_k^{\text{SCMU}}$$

$$\text{s.t.} \quad \text{C1} - \text{C3}. \quad (23)$$

According to (3)–(7), subproblem P2.1 can be rewritten as

$$\textbf{P2.1.1}: \quad \max_{\rho_k^2; \theta_k^1, \dots, \theta_k^N} |(h_k + \mathbf{H}_k \Theta_k \mathbf{G}_k)\rho_k|^2$$

$$\text{s.t.} \quad \text{C1} - \text{C3}. \quad (24)$$

Refer to the existed algorithm which has been proposed in [21], by iteratively optimizing one of ρ_k^2 and θ_k^n with the other one being fixed at each time, subproblem P2.1 can be simplified and transferred to a solved optimization problem.

For the $U_k \to \text{RIS} \to \text{AP}$ link, the optimal phase shift of the RIS element n and the optimal transmit power at U_k are given by

$$\theta_k^{n*} = \arg(h_k \rho_k^*) - \arg(H_k^n) - \arg(G_k^n \rho_k^*) \quad (25)$$

and

$$\rho_k^* = \sqrt{P - P_{\text{RIS}}} \frac{h_k + \mathbf{H}_k \Theta_k^* \mathbf{G}_k}{|h_k + \mathbf{H}_k \Theta_k^* \mathbf{G}_k|} \quad (26)$$

where $\arg(\cdot)$ denotes the componentwise phase of a complex. G_k^n is the channel from U_k to the RIS element n, H_k^n is the channel from the RIS element n to AP. $\Theta_k^* = \text{diag}(e^{j\theta_k^{1*}}, \dots, e^{j\theta_k^{n*}}, \dots, e^{j\theta_k^{N*}})$ denotes the optimal phase shift of the RIS.

2) Fixed RIS Configuration $\Theta_1, \dots, \Theta_K$ and $\rho_1^2, \dots, \rho_K^2$: Problem P2 can be rewritten as a subproblem P2.2

$$\textbf{P2.2}: \quad \max_{r_1, \dots, r_K} \sum_{k=1}^{K} r_k$$

$$\text{s.t.} \quad \text{C4} - \text{C6}. \quad (27)$$

Subproblem P2.2 can be viewed as a mixed integer linear program (MILP) problem that can be solved using the branch-and-bound described as in [42].

V. RIS-ASSISTED MCMU COMMUNICATIONS

In this section, we extend RIS-assisted SCMU communications to RIS-assisted MCMU communications, wherein the C subchannels and the L RIS groups are considered for the multiuser uplink communications system, i.e., $L > 1$ and $C > 1$.

A. Basic Idea

The proposed RIS-assisted MCMU communications are shown in Fig. 6, where the RIS elements can be divided into L groups to support the multiple users' transmissions on the total C subchannels. Phase 1 is for negotiation on the common channel, and Phase 2 is for data transmissions via L RIS groups on C subchannels. Note that the common channel can be divided into C subchannels during Phase 2, and
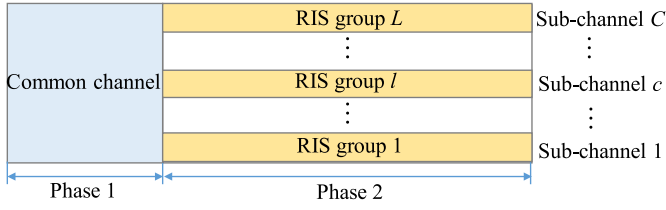
Fig. 6. RIS-assisted MCMU communications, where $L = C > 1$. Phase 1 is for negotiation on the common channel, Phase 2 is for data transmissions via L RIS groups on C subchannels that are divided by the common channel.
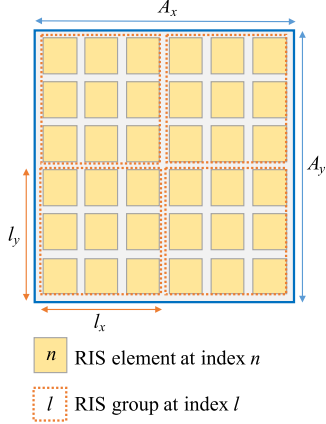

Fig. 7. RIS group division.

$L = C > 1$. Generally, the adjacent RIS elements are combined into one group by prenegotiation (i.e., the eRTS/eCTS exchanging) with the AP on the common channel. Each RIS group can be reserved by the different required users to assist the data transmission on the different subchannels. Different from RIS-assisted SCMU communications, RIS-assisted MCMU communications are presented based on three strategies: 1) the RIS group division; 2) the subchannel allocation; and 3) the four-dimension reservation. It is noted that the RIS group division is combined with the subchannel allocation enabling one RIS group to support one user's transmission on one subchannel. In other words, the reflection coefficients of different RIS groups can be adjusted by the AP for different users to assist multiple data transmissions at a time, thus significantly improving the efficiency of the RIS.

To implement RIS-assisted MCMU communications, we consider three problems: 1) how to divide the RIS group effectively; 2) how to allocate the common channel and the subchannel for negotiation and RIS-assisted transmissions; and 3) how to achieve the four-dimension reservation.

1) RIS Group Division: In this article, a group that the adjacent RIS elements can build a small block is illustrated in Fig. 7. Without loss of generality, suppose that the size of the RIS is A ($A_x : A_y$), and the size of each RIS group is $l(l_x : l_y)$. Let L denote the number of RIS groups, $1 \leq L \leq A$, we have $l = A/L$ (e.g., the elements in the area of $l_x * l_y$ are regarded as one group) and the RIS group ratio is $1/l$. Based on the RIS group division scheme, it is evident that one subchannel can be occupied by one RIS group. The complexity of RIS elements' reflection coefficients updating for one user in RIS-assisted MCMU communications is $\mathcal{O}(N/L)$. Specifically, if

the same reflection coefficient is adopted in one rectangular-shaped group (i.e., each RIS group sets the same reflection coefficient for all the elements included in one RIS group), the AP only needs to adjust the phase shift of each group but not each element. Therefore, the complexity of RIS phase-shift adjustment can be effectively decreased to $\mathcal{O}(1)$.

2) Channel Allocation: To avoid the collision among the different RIS groups, subchannels are used for RIS-assisted transmission, where each subchannel is designated one RIS group (i.e., $L = C$). During the negotiation between user and AP, the eRTS/eCTS transmissions are allowed to execute on the common channel. As the data transmission arrives, the common channel is divided into multiple fixed subchannels, which enables each RIS group to assist the user's transmission. For example, the available bandwidth is B, assuming C subchannels are required for the multiuser uplink communications system; the available bandwidth of each subchannel is B/C. In other words, each RIS group can occupy the B/C (or B/L) bandwidth without interference, and then AP can adjust the phase shift of each RIS group to assist the different users' data transmissions at different subchannels.

3) Four-Dimension Reservation: In RIS-assisted MCMU communications, four-dimension reversion is adopted by the requested user and AP. Each dimension reserved zone is denoted by D1 (r_k), D2 (ρ_k^2), D3 (Θ_k^l), and D4 (c_k, l_k).

1) *User Reservation in Phase 1:* The requested user reserves the resources of the time zone and the channel zone (e.g., r_k and (c_k, l_k) are for the requested user U_k). It is noted that the RIS group can be determined once the subchannel is selected. Besides, the reserved information that is included in the eRTS packet can be directly sent to the AP without the RIS assistance.

2) *AP Reservation in Phase 1:* On receiving the reserved request that includes r_k and (c_k, l_k) information from the requested users, the AP makes the decisions as follows: if the time resource and the subchannel (i.e., the RIS group) are not occupied, the AP computes the optimal transmit power and the optimal reflection coefficient of the reserved RIS group that belongs to the RIS zone. Then, the AP adjusts the phase shift of the reserved RIS group to the optimal value to assist the requested user's data transmission with the optimal power (e.g., Θ_k^l is for the requested user U_k relying on the reserved RIS group l_k with the power ρ_k^2). After this, the reserved information is feedback to the requested user and controller. Otherwise, the AP directly replies to the requested user without the computation of the optimal reflection coefficient.

An illustration of four dimension revision is displayed in Fig. 8. It is assumed that four users (i.e., U_1, U_2, U_3, and U_4) win the negotiation privilege and implement the four-dimension reservation after finishing the backoff, where we set $T_{\text{cycle}} = 4$ slots, $\{r_1, r_2, r_3, r_4\} \in [1, r_{\max}]$. Since the periodic transmission, the reserved values of three zones comprising D2, D3, and D4 are fixed for one user in each RIS-assisted transmission period, and these values may change in the next frame. For example, in a frame, after negotiation with the AP in Phase 1, U_1 reserves its slots set, i.e.,
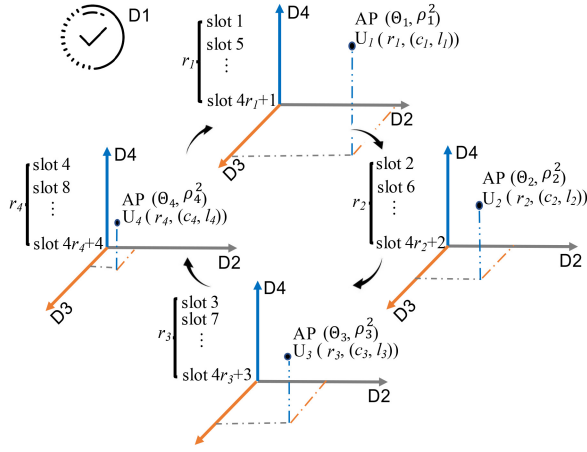
Fig. 8. Illustration of four dimension reversion.

$\{slot\ 1, slot\ 5, \ldots, slot\ 4r_1 + 1\}$. In slot 1, the reflect coefficients of elements that are included in the RIS group l_1 are adjusted as Θ_1, and U_1's transmissions are supported by the RIS group l_1 with power ρ_1^2 on the subchannel c_1. As slot 2 arrives, the reflection coefficients of elements that are included in the RIS group l_2 are adjusted as Θ_2, and U_2's transmissions are supported by the RIS group l_2 with power ρ_2^2 on the subchannel c_2. Similarly, RIS-assisted transmissions can be successfully completed on U_3 and U_4. When a new periodic start, the transmissions relying on the different RIS group are repeated for U_1, U_2, U_3, and U_4, respectively.

B. Implementation Algorithm

Based on the three strategies mentioned above, the implementation algorithm of RIS-assisted MCMU communications is shown in Algorithm 2, where four steps are operated in Phase 1, and three steps are performed in Phase 2.

1) Phase 1 (Negotiation Phase):

1) *Step 1:* U_k wins the access privilege with backoff operation, and negotiates with the AP on the common channel.

2) *Step 2:* By sending an eRTS packet to the AP at the transmit power P, U_k requests T_k^{ini}, r_k, T_{cycle}, c_k for its reserved RIS-assisted transmissions. The other users keep silent by setting NAV when U_k is negotiating with the AP.

3) *Step 3:* Once receiving the eRTS packet from U_k, the AP judges whether the collision happens on the requested channel and time. If not, the AP estimates the RIS group's phase shift and calculates transmit power at U_k. Then, ρ_k^2, T_k^{ini}, r_k, c_k and T_{cycle} are recorded into the eCTS packet and is replied to U_k. The AP also notifies the RIS controller about ϕ_k^l, T_k^{ini}, r_k, c_k, l_k and T_{cycle}. Otherwise, the AP replies U_k without reservation.

4) *Step 4:* Once U_k receiving the eCTS packet from the AP, if RIS group is reserved, U_k ceases its competition and waits for Phase 2. Otherwise, U_k continues its competition and reserves the other RIS group. When the NAV expires, other requested users continue the backoff until Phase 1 terminates.

2) Phase 2 (RIS-Assisted Transmission Phase):

Algorithm 2: RIS-Assisted MCMU Communications

Input: C, L;
Output: ϕ_k^l, ρ_k^2, c_k, l_k, T_k^{ini} and r_k;

1 Initialize $|\phi_k^l| = 0$, $\rho_k^2 = P$, $\forall j, k \in [1, K]$;
2 $t = 0$;
3 **Phase 1: Negotiation on the common channel**;
4 **if** *t is in Phase 1* **then**
5   **if** *U_k has data to transmit AP* **then**
6   U_k sets its backoff value $\{W, s\}$;
7   **if** $W = 0$ **then**
8   U_k sends eRTS to AP;
9        $U_{j,j \neq k}$ sets NAV and keeps silent;
10   AP receives eRTS packet and judges;
11   **if** *no collisions* **then**
12   AP calculates ϕ_k^l, ρ_k^2, l_k;
13   AP replies eCTS to U_k;
14   AP notifies the RIS controller about ϕ_k^l, l_k, r_k, c_k, T_k^{ini}, T_{cycle};
15   **end**
16   **else**
17   AP replies eCTS without reservation;
18   **end**
19   U_k receives eCTS packet and waits for **Phase 2** arriving;
20   **end**
21   **else**
22        $W - -$;
23   **end**
24   **end**
25   **else**
26   U_k keeps silent;
27   **end**
28 **end**
29 **else**
30   U_k waits for **Phase 1** arriving;
31 **end**
32 **Phase 2: RIS-assisted transmission on L groups and C sub-channels**;
33 **if** *t is in Phase 2* **then**
34   U_k transmits its data with power, ρ_k^2, on the reserved sub-channel in the reserved slots;
35   The RIS controller sets ϕ_k^l for the RIS group l_k;
36   The RIS group l_k adjusts its phase-shift to reflect U_k's signal to AP on the sub-channel c_k;
37   AP receives the signals from the RIS group l_k and the LOS path on the sub-channel c_k;
38   AP replies an ACK packet to U_k;
39 **end**
40 **else**
41   U_k waits for **Phase 2** arriving;
42 **end**

---

1) *Step 1:* As Phase 2 arrives, U_k sends the data with the transmit power ρ_k^2. Meanwhile, the RIS controller sets the phase shift of the reserved RIS group as $\theta_k^{l(n)}$, and the

RIS group assists U_k's data transmission at the reserved subchannel and the reserved slots.

2) *Step 2:* Once the AP receives the accumulated reflected signal from the RIS group and the LOS's signals from U_k, the AP replies an ACK packet to U_k.

3) *Step 3:* When the reserved RIS-assisted transmissions between U_k and AP commence, the other users that reserve the same RIS group set NAV to cease their transmissions until the reserved RIS-assisted transmissions of U_k finishes. It is noted that the other users can continue RIS-assisted transmissions on the other RIS group without keeping silent.

C. Performance Analysis

According to the performance analysis in Section IV-B, the proposed Markov model is available for the subchannel as well. According to (14) and (15), $\tau_j, j \in [1, C]$ that the stationary probability that one user U_k transmits a data packet in a random slot when j subchannels are used is provided in (28), shown at the bottom of the page.

Recalling (13), the value of q_j and p_j can be expressed as

$$q_j = \frac{\eta_j}{\gamma_j + \eta_j} \tag{29}$$

and

$$p_j = 1 - \left(1 - \tau_j\right)^{Kq_j - 1} \tag{30}$$

where q_j and p_j denote the probability of a user U_k stays in the "C" state when j subchannels are used simultaneously, and the probability that a collision occurs on the common channel when j subchannels can be used, respectively, K is the number of users in the network.

According to queuing model [43], the value of γ_j and η_j can be obtained as

$$\eta_j = j\eta \tag{31}$$

and

$$\gamma_j = \frac{\zeta_s^j}{\zeta_e^j \delta + \zeta_s^j t_s + \zeta_c^j t_c} \tag{32}$$

where the value of η is given in (16).

Therefore, as the single-channel is extended to j subchannels, the probability of successful transmission (ζ_s^j), the probability of idle channel (ζ_e^j) and the probability of collision (ζ_c^j) can be, respectively, given as

$$\begin{cases} \zeta_s^j = Kq_j\tau_j\left(1 - \tau_j\right)^{Kq_j - 1} \\ \zeta_e^j = \left(1 - \tau_j\right)^{Kq_j} \\ \zeta_c^j = 1 - \zeta_s^j - \zeta_e^j. \end{cases} \tag{33}$$

For RIS-assisted MCMU communications, the process that U_k accesses the subchannel after contending with other users on the common channel is regarded as an $M/M/C$ queuing model [44], [45], where the U_k successfully contending will be served via one of the C subchannels. Let $\nu(t)$ denote the number of used subchannels at time t, and the steady-state probability $\pi(j)$ with exactly j number of used subchannels is defined as

$$\pi_j = \lim_{t \to \infty} P\{\nu(t) = j\} \quad j \geq 0. \tag{34}$$

Based on the two-state Markov chain model, it is known that a user accesses the subchannel with the rate γ_j when j subchannels are used, $j \in [1, C]$. Since $\sum_{j=1}^{K} \pi_j = 1$, and then the steady-state probability π_j is calculated as

$$\pi_j = \frac{\frac{\prod_{l=0}^{j-1} \gamma_l}{\eta^j j!}}{\sum_{i=1}^{C} \frac{\prod_{l=0}^{i-1} \gamma_l}{\eta^i i!} + 1}, \quad j = 1, \ldots, C. \tag{35}$$

Given the achievable data rate at each user U_k, $R_k^{\text{MCMU}}(\rho_k, \phi_k) = (B/C) \log_2(1 + \text{SNR}_k^{\text{MCMU}})$. The total capacity of RIS-assisted MCMU communications on all subchannels can be calculated as follows:

$$\begin{aligned} \mathfrak{I}_{\text{Total}}^{\text{MCMU}} &= \sum_{j=1}^{C} \sum_{k=1}^{K} \frac{t_p r_k}{T} \varepsilon_k^j \pi_j R_k^{\text{MCMU}}(\rho_k, \phi_k) \\ &= \frac{t_p t_h B}{T t_s K C} \sum_{j=1}^{C} \zeta_s^j \pi_j \sum_{k=1}^{K} r_k \log_2\left(1 + \text{SNR}_k^{\text{MCMU}}\right) \end{aligned} \tag{36}$$

where $\varepsilon_k^j = ([t_h \zeta_s^j]/t_s K)$ is the probability that U_k transmits data in Phase 2 when j subchannels are used.

D. Performance Optimization

To maximize the system capacity in (36). The performance optimization of RIS-assisted MCMU communications can be separately operated at the AP and users. Specifically, the AP executes the phase-shift optimization of the reserved RIS group for the requested users, and the requested users complete the optimization of subchannel selection and the number of reserved transmissions. Both of them are formulated in problems P3 and P4, respectively.

1) Phase-Shift and the Transmit Power Optimization by AP: Problem P3 is formulated to solve the optimal phase shift of each RIS group as

$$\textbf{P3}: \max_{\rho_1^2, \ldots, \rho_K^2; \phi_1^{l(n)}, \ldots, \phi_K^{l(n)}} \sum_{k=1}^{K} \log_2\left(1 + \text{SNR}_k^{\text{MCMU}}\right)$$

$$\textbf{s.t.} \quad \text{C7}: \quad 0 \leq \rho_k^2 \leq P - \frac{1}{L}P_{\text{RIS}} \quad \forall k$$

$$\text{C8}: \quad |\phi_k^{l(n)}| = 1, \quad n \in l \quad \forall k, l$$

$$\text{C9}: \quad \theta_k^{l(n)} \in \boldsymbol{\Omega}, \quad n \in l \quad \forall k, l$$

$$\text{C10}: \quad 1 \leq l \leq L, \quad L = C \tag{37}$$

$$\tau_j = \frac{2(1 - 2p_j)q_j}{q_j\left[(W + 1)(1 - 2p_j) + p_j W\left(1 - (2p_j)^m\right)\right] + 2(1 - q_j)(1 - p_j)(1 - 2p_j)} \tag{28}$$

where C7 constrains the transmit power of each user when L RIS groups can be used. Constraints C8 and C9 separately give the constraints of the amplitude and phase shift of the RIS group for each user. Constraint C10 illustrates the feasibility constraints.

To solve problem P3, we can maximize the SNR of each user by adjusting the phase shift of the selected RIS group. According to (3)–(7), problem P3 can be simplified as problem P3.1, which is shown as

$$\textbf{P3.1}: \quad \max_{\rho_k^2; \theta_k^{l(n)}} \left| \left(h_k + \mathbf{H}_k^l \mathbf{\Theta}_k^l \mathbf{G}_k^l \right) \rho_k \right|^2$$
$$\text{s.t.} \quad \text{C7} - \text{C10} \tag{38}$$

where G_k^l and H_k^l are the channel from U_k to the RIS group l, and reflect to AP, $\mathbf{\Theta}_k^l$ is the reflection coefficient of the RIS group l.

Refer to the existed algorithm which has been proposed in [21], by iteratively optimizing one of ρ_k^2 and $\theta_k^{l(n)}$ with the other one being fixed at each time, the optimal phase shift of the nth element on the RIS group l and the optimal transmit power at U_k can be given as

$$\theta_k^{l(n)^*} = \arg\left(h_k \rho_k^*\right) - \arg\left(H_k^{l(n)}\right) - \arg\left(G_k^{l(n)} \rho_k^*\right) \tag{39}$$

and

$$\rho_k^* = \sqrt{P - \frac{1}{L} P_{\text{RIS}}} \frac{h_k + \mathbf{H}_k^l \mathbf{\Theta}_k^{l^*} \mathbf{G}_k^l}{\left| h_k + \mathbf{H}_k^l \mathbf{\Theta}_k^{l^*} \mathbf{G}_k^l \right|} \tag{40}$$

where $G_k^{l(n)}$ is the channel from U_k to the RIS element n on the group l, $H_k^{l(n)}$ is the channel from the RIS element n on the group l to AP. $\mathbf{\Theta}_k^{l^*} = \text{diag}(e^{j\theta_k^{1^*}}, \dots, e^{j\theta_k^{n^*}}, \dots, e^{j\theta_k^{L^*}})$. With considering a same reflect coefficient for all elements in the RIS group l, we have $G_k^{l(n)} = G_k^l, H_k^{l(n)} = H_k^l$, and $\theta_k^{l^*} = \theta_k^{l(n)^*} \; \forall n \in l$, where G_k^l is the channel from U_k to the RIS group l, H_k^l is the channel from the RIS group l to AP. Thus, the optional phase shift in (39) for the RIS group l can be rewritten as

$$\theta_k^{l^*} = \arg\left(h_k \rho_k^*\right) - \arg\left(H_k^l\right) - \arg\left(G_k^l \rho_k^*\right). \tag{41}$$

2) Number of Reserved Transmissions Optimization by User With Subchannel Selection: since each user is able to obtain the state of each subchannel (e.g., the subchannel is reserved or not) by performing eRTS/eCTS exchanging with AP. Let $V(c_k)$ represent the subchannel c_k can be reserved by the U_k or not. In other words, if U_k successfully reserves one subchannel c_k, $V(c_k) = 1$; Otherwise, $V(c_k) = 0$. The problem formulation at each user can be formulated as

$$\textbf{P4}: \quad \max_{c_1, \dots, c_K; r_1 \dots, r_k} \frac{t_p t_h B}{T t_s K C} \sum_{j=1}^{C} \zeta_s^j \pi_j \sum_{k=1}^{K} r_k$$

$$\text{s.t. C4, C6}$$
$$\text{C11}: \quad \frac{t_p}{t_s} r_{\max} \zeta_s^C \leq \frac{t_r}{t_h}$$
$$\text{C12}: \quad \sum_{k=1}^{K} V(c_k) = t_h \zeta_s^C / t_s \; \forall k$$
$$\text{C13}: \quad V(c_k) \in \{0, 1\} \quad \forall k$$
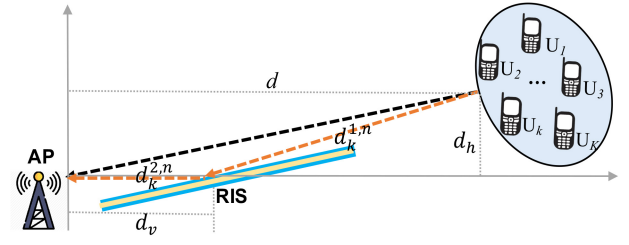

Fig. 9. Simulated RIS-assisted communications scenario.

$$\text{C14}: \quad 1 \leq c_k \leq C, C = L \quad \forall k \tag{42}$$

where C11 constrains the RIS-assisted transmission period and the negotiation period when C subchannels can be used. Constraints C12 and C13 constrain the number of subchannels for users.

Since $([t_p t_h B]/T t_s K C) \sum_{j=1}^{C} \zeta_s^j \pi_j$ is a constant when the number of subchannels is given, problem P4 can be rewritten as problem P4.1

$$\textbf{P4.1}: \quad \max_{c_1, \dots, c_K; r_1, \dots, r_K} \sum_{k=1}^{K} r_k$$
$$\text{s.t.} \quad \text{C4, C6, C11-C14.} \tag{43}$$

Subproblem P4.1 can be viewed as a MILP problem that can be solved using the branch-and-bound described as in [42].

VI. PERFORMANCE EVALUATION

In this section, given a fixed RIS location, we evaluate the performance RIS-assisted MAC with NS-2.35 simulator. Besides, the SimRIS simulator can be used for the RIS evaluation under considering the RIS location [46]. RIS-assisted multiuser uplink communications system scenario comprising one AP, one RIS and 100 users is considered. To simplify the simulation, we assume that all users are with the close position so as to achieve the same SNR at the AP, as shown Fig. 9. Wherein $d_k^{1,n} = \sqrt{d_h^2 + (d - d_v)^2}$, $d_k^{2,n} = d_h = 2$ m, and $d_v = 5$ m. The critical parameters are given as follows: the length of one frame, the time duration of one data transmission, and the transmission cycle are set to be $T = 200$ ms, $t_h = 20$ ms, $t_p = 0.5$ ms, $T_{\text{cycle}} = 18$ data transmissions, and $r_{\max} = 20$, respectively. The packet size of eRTS and eCTS are set to be 24 bytes and 16 bytes, respectively. SIFS and DIFS are set to be 10 and 50 μs, respectively. The minimum contention window W_0 is set to be 15, and the maximum backoff stage m is set to be 6. The bandwidth is set to be $B = 10$ Mb/s, the operating frequency is set to be $f_c = 5$ GHz. The number of RIS elements is set to be $N = 128$, i.e., $L = 1$ and $A(16:8)$. For RIS-assisted MCMU communications, L is valued as $2, 4, 8, 16$, where the size of RIS group are set to be $l(8:8)$, $l(8:4)$, $l(4:4)$, $l(4:2)$, respectively. Other required parameters for each user (e.g., U_k) are set to be $d = 60$ m, $\sigma^2 = -80$ dBm, and $P = 5$ dBm (if not specified otherwise).

A. Numerical Results

In Fig. 10, the numerical results of RIS-assisted SCMU communications are evaluated in terms of SNR, transmit
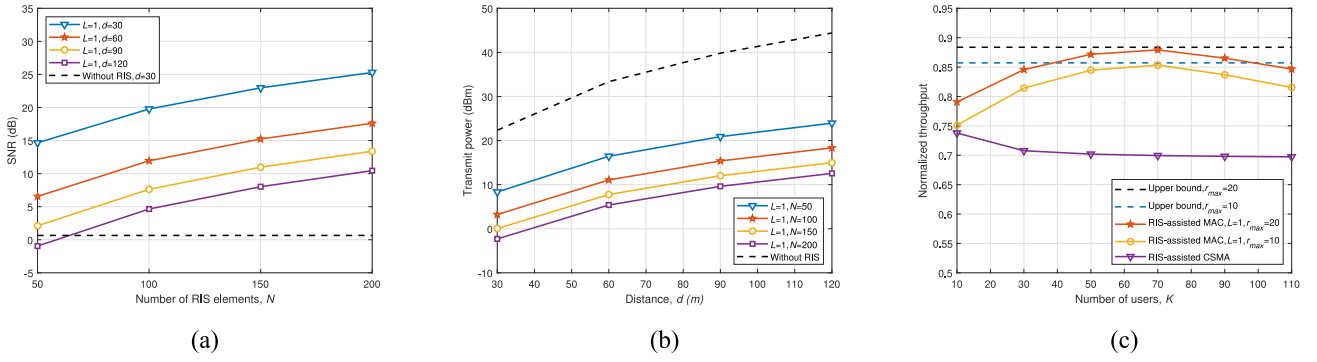
Fig. 10. Numerical evaluation of RIS-assisted SCMU communications in terms of SNR, transmit power, and normalized throughput. (a) SNR versus number of RIS elements. (b) Transmit power versus distance. (c) Normalized throughput versus number of users.
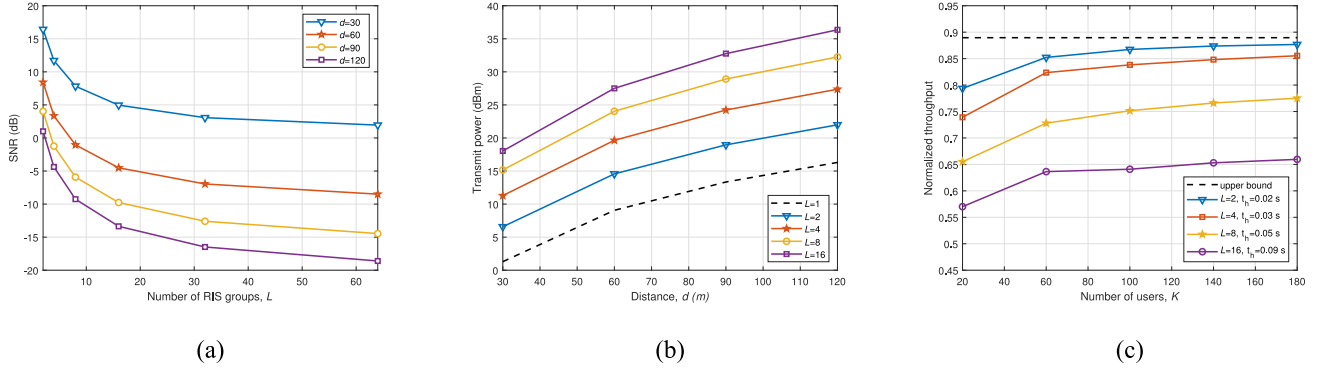

Fig. 11. Numerical evaluation of RIS-assisted MCMU communications in terms of SNR, transmit power, and normalized throughput. (a) SNR versus number of RIS groups. (b) Transmit power versus distance. (c) Normalized throughput versus number of users.

power, and normalize throughput. Specifically, Fig. 10(a) shows the received SNR at the AP versus the number of RIS elements with the different distances between the user and AP. It is observed that the received SNR is increasing with N, and it has significant improvement compared with the scheme without RIS. Besides, the received SNR is enhanced when the user is closer to the AP (e.g., the received SNR becomes better as the distance decreases from 120 m to 30 m). Fig. 10(b) shows the transmit power at user versus the distance between the user and AP with the different number of RIS elements. It can be seen that the transmit power at user increases with d, and decreases with N. Compared to the scheme without RIS, the user's transmit power using the RIS can be decreased significantly, and thus the energy efficient is achieved in the multiuser uplink communications system. Fig. 10(c) shows the normalized throughput versus the number of users. As the optimal phase shift of each RIS element is solved by the AP to support the uplink traffic of each user, RIS-assisted SCMU communications can achieve better throughput performance compared with RIS-assisted CSMA scheme, where RIS-assisted CSMA scheme denotes RIS-assisted transmissions using the conventional CSMA/CA scheme. This is because the negotiation of the RIS resources can avoid interference caused by the RIS reflection. Besides, the throughput performance can be improved as r_{max} is increasing, this is because the increasing of negotiation efficiency. And the upper bounds are given in terms of the different r_{max}.

In Fig. 11, the numerical results of RIS-assisted MCMU communications are evaluated in terms of SNR, transmit power, and normalize throughput. Specifically, Fig. 11(a) shows the received SNR at AP versus the number of RIS groups with the different distances between the user and AP. It can be seen that the received SNR decreases with L and d, respectively. Compared to RIS-assisted SCMU communications, the SNR of RIS-assisted MCMU communications is not only affected by the distance and but also by the number of RIS groups. Therefore, the SNR of RIS-assisted MCMU communications is lower than RIS-assisted SCMU communications. Fig. 11(b) shows the transmit power at user versus the distance between the user and AP under the different numbers of RIS groups and subchannels. It is shown that the transmit power at user increases with d and L. Compared with RIS-assisted SCMU communications, the transmit power at the user with RIS group division is improved because that the reflecting elements are divided into the different RIS groups to support the different user's communication at the same time. It indicates that the fewer RIS groups, the less energy consumption. Fig. 11(c) shows the received SNR at AP versus the number of RIS groups under the different distances between the user and AP. It can be seen that the received SNR decreases with L and d, respectively. Besides, the higher SNR can be gained in RIS-assisted SCMU communications compare to RIS-assisted MCMU communications with the RIS group division. As L increases from 2 to 16, the normalized throughput decreases from 0.88 to about 0.65 after saturation and below
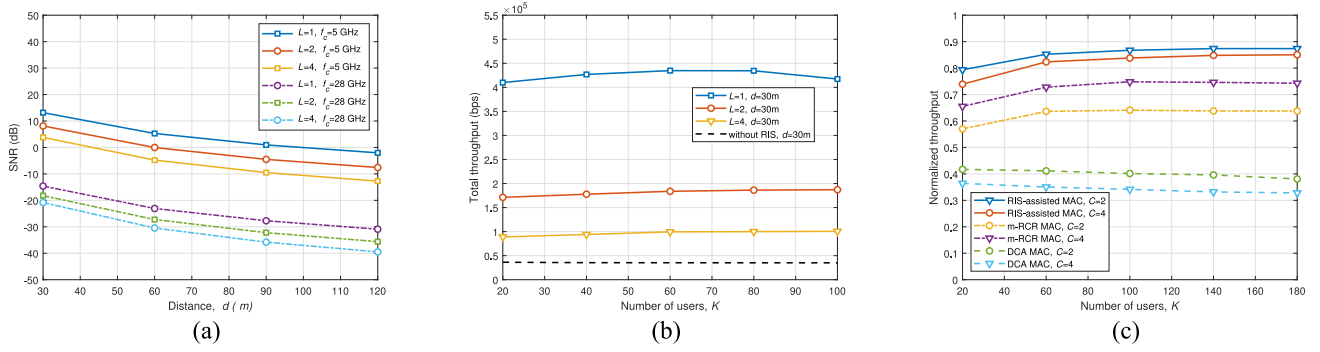
Fig. 12. Simulation evaluation of RIS-assisted SCMU/MCMU communications with the different operation frequency, and the various schemes. (a) SNR versus distance. (b) Total throughput versus number of users, $f_c = 28$ GHz. (c) Normalized throughput versus number of users, $f_c = 5$ GHz.
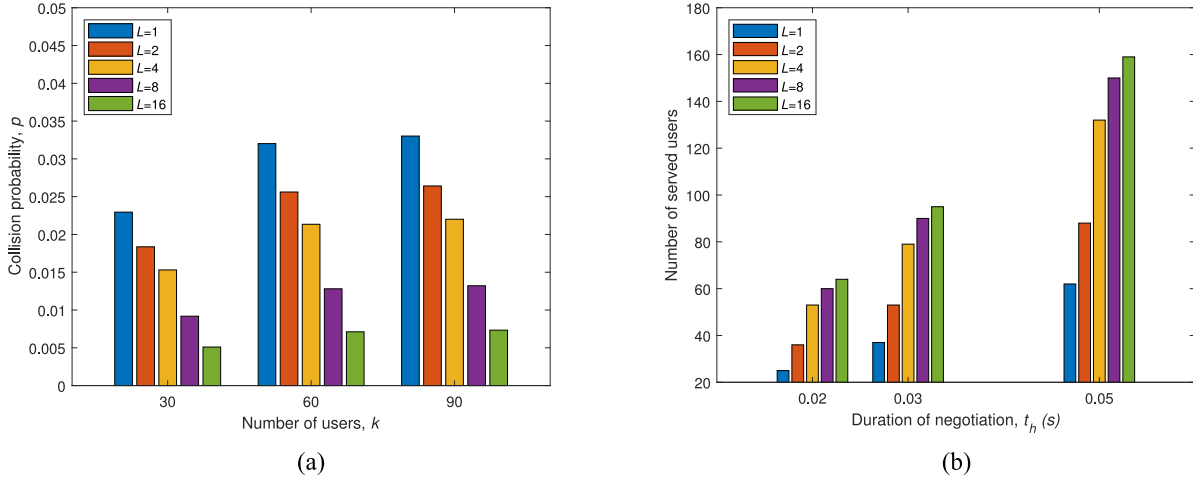

Fig. 13. Simulation evaluation of RIS-assisted SCMU/MCMU communications in terms of collision probability and the number of served users. (a) Collision probability versus number of users. (b) Number of served users versus negotiation period, where $K = 300$.

the upper bound. It is observed that the value of t_h increases with the L and K, this is because the more RIS groups are used to support users' communications, then, the longer duration of the negotiation period is required. Intuitively, the overhead can be quantized as $t_h/(t_h + t_r) = 1/(1 + t_r/t_h)$. It can be observed that the overhead increases with the ratio of t_r/t_h decreasing. It brings a higher negotiation overhead and leads to a lower transmission efficiency. Therefore, the ratio of t_r/t_h can be dynamically adjusted to control the overhead and the real-time transmission.

B. Simulation Results

In Fig. 12, simulation evaluations of RIS-assisted SCMU/MCMU communications on the different operating frequencies and the various schemes are given. Fig. 12(a) evaluates the impact of operating frequency on RIS-assisted communications system, where the operating frequency is set to be 5 and 28 GHz, respectively, the number of RIS groups is set to be 1, 2, and 4, respectively. It is shown that the SNR significantly decreases when the operating frequency increases to mmWave frequency due to the severe channel propagation loss. Besides, the similar trends that have been verified in Fig. 11(a) demonstrate the relationship among SNR, L, and d in RIS-assisted SCMU/MCMU communications (i.e., the better received SNR the lower L and d). Fig. 12(b) shows the

total throughput in mmWave frequency (i.e., $f_c = 28$ GHz), where the total throughput of RIS-assisted mmWave communications first increases and then slightly declines as the number of users increases. Compared with the typical mmWave communications without RIS, the performance of RIS-assisted mmWave communications for each user can be improved up to 50% when the number of RIS groups is set to be 1. Fig. 12(c) shows the performance comparison among the different multichannel MAC protocols in 5 GHz frequency, where m-RCR MAC protocol [47] and DCA MAC protocol [48] are the benchmarks. Compared with m-RCR MAC and DCA MAC, the proposed RIS-assisted MAC performs the best due to the MDR scheme. In particular, due to the limitation of the negotiation phase in the proposed RIS-assisted MAC, the normalized throughput increases and then keeps almost unchanged as the number of users increases. The performance of m-RCR MAC is better than DCA since the channel reservation is used, and its performance improves with the number of data channels increasing before the control channel saturation. However, its performance keeps almost constant even after the control channel saturation. The DCA MAC performs the worst due to its bottleneck of the control channel, and its channel utilization decreases with the number of data channels after the control channel saturation.

In Fig. 13, simulation evaluations of RIS-assisted SCMU/MCMU communications in terms of the collision probability and the number of served users are presented. Fig. 13(a) shows the collision probability versus the number of users. It is observed that the collision probability first obviously increases and then slightly climbs as the number of users increases. This is because the collision probability is also affected by the probability that a user is staying at the "C" state besides the number of users. Moreover, the collision probability also decreases as the number of RIS groups increases due to more users are allowed for accessing at a time. Fig. 13(b) shows the number of served users versus the duration of the negotiation period in RIS-assisted MCMU communications with a different number of RIS groups, where $K = 300$. When the duration of the negotiation period is separately set to be 0.02, 0.03, and 0.05 s, with the negotiation period enlarging, the more users can be served. Also, the more RIS groups are divided, the more users communicate with AP. Compared with RIS-assisted SCMU communications, RIS-assisted MCMU communications can serve more users, although the system throughput may be decreased. Therefore, there is a tradeoff between the system throughput and the served number of users.

VII. Conclusion

This article investigated how to utilize the RIS to assist the multiuser uplink communications system and increase the system's coverage and rate with the power constraint. We proposed an RIS-assisted MAC framework. With this design, RIS-assisted SCMU/MCMU communications were presented, respectively. In particular, RIS-assisted SCMU/MCMU communications can be implemented by two separate phases: 1) the negotiation phase and 2) the RIS-assisted transmission phase. Before RIS-assisted data transmissions, the time slots, the transmit power, the RIS elements, and even the subchannel can be negotiated in advance. In both cases, RIS elements viewed as the reserved resources can be served for uplink traffics based on the prenegotiation. It is thereby avoiding interference caused by the RIS reflection and decreasing energy consumption. Besides, RIS-assisted MCMU communications can reduce the RIS computation complexity compared to RIS-assisted SCMU communications. Numerical results on RIS-assisted SCMU/MCMU communications shown that RIS-assisted SCMU communications can gain better throughput, and RIS-assisted MCMU communications can serve more users, and both of them can decrease the transmit power.

In future work, we will address the distributed optimization issues in RIS-assisted networks considering user location. Besides, as the RIS technology is developed in mmWave/THz communications [46], [49], designing RIS-assisted MAC in mmWave/THz frequency is a potential challenge.

Acknowledgment

References

[1] K. B. Letaief, W. Chen, Y. Shi, J. Zhang, and Y.-J. A. Zhang, "The roadmap to 6G: AI empowered wireless networks," *IEEE Commun. Mag.*, vol. 57, no. 8, pp. 84–90, Aug. 2019.

[2] W. Saad, B. Mehdi, and M. Chen, "A vision of 6G wireless systems: Applications, trends, technologies, and open research problems," *IEEE Netw.*, vol. 34, no. 3, pp. 134–142, May/Jun. 2020.

[3] A. Aijaz, "Private 5G: The future of industrial wireless," *IEEE Ind. Electron. Mag.*, vol. 14, no. 4, pp. 136–145, Dec. 2020.

[4] A. Aijaz, "High-performance industrial wireless: Achieving reliable and deterministic connectivity over IEEE 802.11 WLANs," *IEEE Open J. Ind. Electron. Soc.*, vol. 1, pp. 28–37, Mar. 2020.

[5] C. Huang *et al.*, "Holographic MIMO surfaces for 6G wireless networks: Opportunities, challenges, and trends," *IEEE Wireless Commun.*, vol. 27, no. 5, pp. 118–125, Oct. 2020.

[6] C. Huang, R. Mo, and C. Yuen, "Reconfigurable intelligent surface assisted multiuser MISO systems exploiting deep reinforcement learning," *IEEE J. Sel. Areas Commun.*, vol. 38, no. 8, pp. 1839–1850, Aug. 2020.

[7] M. Di Renzo *et al.*, "Reconfigurable intelligent surfaces vs. relaying: Differences, similarities, and performance comparison," *IEEE Open J. Commun. Soc.*, vol. 1, pp. 798–807, 2020.

[8] M. A. ElMossallamy, H. Zhang, L. Song, K. G. Seddik, Z. Han, and G. Y. Li, "Reconfigurable intelligent surfaces for wireless communications: Principles, challenges, and opportunities," *IEEE Trans. Cogn. Commun. Netw.*, vol. 6, no. 3, pp. 990–1002, Sep. 2020.

[9] M. D. Renzo *et al.*, "Smart radio environments empowered by reconfigurable intelligent surfaces: How it works, state of research, and the road ahead," *IEEE J. Sel. Areas Commun.*, vol. 38, no. 11, pp. 2450–2525, Nov. 2020.

[10] S. V. Hum and J. Perruisseau-Carrier, "Reconfigurable reflectarrays and array lenses for dynamic antenna beam control: A review," *IEEE Trans. Antennas Propag.*, vol. 62, no. 1, pp. 183–198, Jan. 2014.

[11] Q.-Ul-A. Nadeem, H. Alwazani, A. Kammoun, A. Chaaban, M. Debbah, and M.-S. Alouini, "Intelligent reflecting surface-assisted multi-user MISO communication: Channel estimation and beamforming design," *IEEE Open J. Commun. Soc.*, vol. 1, pp. 661–680, 2020.

[12] M. D. Renzo *et al.*, "Smart radio environments empowered by reconfigurable AI meta-surfaces: An idea whose time has come," *EURASIP J. Wireless Commun. Netw.*, vol. 2019, no. 1, pp. 1–20, Dec. 2019.

[13] B. Di, H. Zhang, L. Song, Y. Li, Z. Han, and H. V. Poor, "Hybrid beamforming for reconfigurable intelligent surface based multi-user communications: Achievable rates with limited discrete phase shifts," *IEEE J. Sel. Areas Commun.*, vol. 38, no. 8, pp. 1809–1822, Aug. 2020.

[14] R. Mehrotra *et al.*, "3D channel modeling and characterization for hypersurface empowered indoor environment at 60 GHz millimeter-wave band," in *Proc. IEEE SPECTS*, Berlin, Germany, 2019, pp. 1–6.

[15] Z. Li *et al.*, "Towards programming the radio environment with large arrays of inexpensive antennas," in *Proc. NSDI USENIX Symp.*, Boston, MA, USA, 2019, pp. 285–300.

[16] S. Hu, F. Rusek, and O. Edfors, "Beyond massive MIMO: The potential of data transmission with large intelligent surfaces," *IEEE Trans. Signal Process.*, vol. 66, no. 10, pp. 2746–2758, Mar. 2018.

[17] E. Basar, "Reconfigurable intelligent surface-based index modulation: A new beyond MIMO paradigm for 6G," *IEEE Trans. Commun.*, vol. 68, no. 5, pp. 3187–3196, May 2020.

[18] E. Basar, "Transmission through large intelligent surfaces: A new frontier in wireless communications," in *Proc. IEEE EuCNC*, Valencia, Spain, 2019, pp. 112–117.

[19] H. Zhang, B. Di, L. Song, and Z. Han, "Reconfigurable intelligent surfaces assisted communications with limited phase shifts: How many phase shifts are enough?" *IEEE Trans. Veh. Technol.*, vol. 69, no. 4, pp. 4498–4502, Apr. 2020.

[20] B. Di, H. Zhang, L. Li, L. Song, Y. Li, and Z. Han, "Practical hybrid beamforming with finite-resolution phase shifters for reconfigurable intelligent surface based multi-user communications," *IEEE Trans. Veh. Technol.*, vol. 69, no. 4, pp. 4565–4570, Apr. 2020.

[21] Q. Wu and R. Zhang, "Intelligent reflecting surface enhanced wireless network: Joint active and passive beamforming design," in *Proc. IEEE GLOBECOM*, Abu Dhabi, United Arab Emirates, 2018, pp. 1–6.

[22] H. Guo, Y.-C. Liang, J. Chen, and E. G. Larsson, "Weighted sum-rate maximization for reconfigurable intelligent surface aided wireless networks," *IEEE Trans. Wireless Commun.*, vol. 19, no. 5, pp. 3064–3076, May 2020.

[23] C. Huang, A. Zappone, G. C. Alexandropoulos, M. Debbah, and C. Yuen, "Reconfigurable intelligent surfaces for energy efficiency in wireless communication," *IEEE Trans. Wireless Commun.*, vol. 18, no. 8, pp. 4157–4170, Aug. 2019.

[24] C. Huang, A. Zappone, M. Debbah, and C. Yuen, "Achievable rate maximization by passive intelligent mirrors," in *Proc. IEEE ICASSP*, Calgary, AB, Canada, 2018, pp. 3714–3718.

[25] C. Huang, G. C. Alexandropoulos, A. Zappone, M. Debbah, and C. Yuen, "Energy efficient multi-user MISO communication using low resolution large intelligent surfaces," in *Proc. IEEE GLOBECOM Workshops*, Abu Dhabi, United Arab Emirates, 2018, pp. 1–6.

[26] S. Abeywickrama, R. Zhang, Q. Wu, and C. Yuen, "Intelligent reflecting surface: Practical phase shift model and beamforming optimization," *IEEE Trans. Commun.*, vol. 68, no. 9, pp. 5849–5863, Sep. 2020.

[27] Y. Han, W. Tang, S. Jin, C.-K. Wen, and X. Ma, "Large intelligent surface-assisted wireless communication exploiting statistical CSI," *IEEE Trans. Veh. Technol.*, vol. 68, no. 8, pp. 8238–8242, Aug. 2019.

[28] A. Taha, M. Alrabeiah, and A. Alkhateeb, "Deep learning for large intelligent surfaces in millimeter wave and massive MIMO systems," in *Proc. IEEE GLOBECOM*, Waikoloa, HI, USA, 2019, pp. 1–6.

[29] B. Yang, X. Cao, C. Huang, C. Yuen, L. Qian, and M. D. Renzo, "Intelligent spectrum learning for wireless networks with reconfigurable intelligent surfaces," *IEEE Trans. Veh. Technol.*, early access, Mar. 5, 2021, doi: 10.1109/TVT.2021.3064042.

[30] X. Yu, D. Xu, Y. Sun, D. W. K. Ng, and R. Schober, "Robust and secure wireless communications via intelligent reflecting surfaces," *IEEE J. Sel. Areas Commun.*, vol. 38, no. 11, pp. 2637–2652, Nov. 2020.

[31] L. Dai *et al.*, "Reconfigurable intelligent surface-based wireless communications: Antenna design, prototyping, and experimental results," *IEEE Access*, vol. 8, pp. 45913–45923, 2020.

[32] A. Aijaz and A. H. Aghvami, "A PRMA based MAC protocol for cognitive machine-to-machine communications," in *Proc. IEEE ICC*, Budapest, Hungary, 2013, pp. 2753–2758.

[33] N. Shahin, R. Ali, and Y.-T. Kim, "Hybrid slotted-CSMA/CA-TDMA for efficient massive registration of IoT devices," *IEEE Access*, vol. 6, pp. 18366–18382, 2018.

[34] Y. Liu, C. Yuen, X. Cao, N. U. Hassan, and J. Chen, "Design of a scalable hybrid MAC protocol for heterogeneous M2M networks," *IEEE Internet Things J.*, vol. 1, no. 1, pp. 99–111, Feb. 2014.

[35] E. Basar, M. D. Renzo, J. De Rosny, M. Debbah, M.-S. Alouini, and R. Zhang, "Wireless communications through reconfigurable intelligent surfaces," *IEEE Access*, vol. 7, pp. 116753–116773, 2019.

[36] I. Yildirim, A. Uyrus, E. Basar, and I. F. Akyildiz, "Propagation modeling and analysis of reconfigurable intelligent surfaces for indoor and outdoor applications in 6G wireless systems," Nov. 2020. [Online]. Available: arXiv:1912.07350.

[37] C. You, B. Zheng, and R. Zhang, "Channel estimation and passive beamforming for intelligent reflecting surface: Discrete phase shift and progressive refinement," *IEEE J. Sel. Areas Commun.*, vol. 38, no. 11, pp. 2604–2620, Nov. 2020.

[38] L. Wei, C. Huang, G. C. Alexandropoulos, and C. Yuen, "Parallel factor decomposition channel estimation in RIS-assisted multi-user MISO communication," in *Proc. IEEE SAM Workshop*, Hangzhou, China, 2020, pp. 1–5.

[39] B. Yang, X. Cao, Z. Han, and L. Qian, "A machine learning enabled MAC framework for heterogeneous Internet-of-Things networks," *IEEE Trans. Wireless Commun.*, vol. 18, no. 7, pp. 3697–3712, Jul. 2019.

[40] X. Cao, B. Yang, and Z. Song, "Performance analysis of hybrid MAC scheme with multi-slot reservation," *Electron. Lett.*, vol. 54, no. 4, pp. 250–252, Feb. 2018.

[41] G. Bianchi, "Performance analysis of the IEEE 802.11 distributed coordination function," *IEEE J. Sel. Areas Commun.*, vol. 18, no. 3, pp. 535–547, Mar. 2000.

[42] S. Boyd, S. P. Boyd, and L. Vandenberghe, *Convex Optimization*. Cambridge, U.K.: Cambridge Univ. Press, 2004.

[43] H. Bobarshad and M. Shikh-Bahaei, "M/M/1 queuing model for adaptive cross-layer error protection in WLANs," in *Proc. IEEE WCNC*, Budapest, Hungary, 2009, pp. 1–6.

[44] B. Yang, B. Li, Z. Yan, and M. Yang, "A channel reservation based cooperative multi-channel MAC protocol for the next generation WLAN," *Wireless Netw.*, vol. 24, no. 2, pp. 627–646, Feb. 2018.

[45] R. Cooper, *Introduction to Queueing Theory. 1981*, Edward Arnold, London, U.K., 2004.

[46] E. Basar, I. Yildirim, and I. F. Akyildiz, "SimRIS channel simulator for reconfigurable intelligent surface-empowered communication systems," 2020. [Online]. Available: arXiv:2006.00468.

[47] B. Yang, B. Li, Z. Yan, D.-J. Deng, and M. Yang, "Performance analysis of multi-channel MAC with single transceiver for the next generation WLAN," *J. Netw. Comput. Appl.*, vol. 146, Nov. 2019, Art. no. 102408.

[48] S.-L. Wu, C.-Y. Lin, Y.-C. Tseng, and J.-L. Sheu, "A new multi-channel MAC protocol with on-demand channel assignment for multi-hop mobile ad hoc networks," in *Proc. IEEE I-SPAN*, Dallas, TX, USA, 2000, pp. 232–237.

[49] C. Huang *et al.*, "Hybrid beamforming for RIS-empowered multi-hop terahertz communications: A DRL-based method," in *Proc. IEEE Globecom*, Taipei, Taiwan, Dec. 2020, pp. 1–6.